Journal Homepage: -www.journalijar.com

INTERNATIONAL JOURNAL OF ADVANCED RESEARCH (IJAR)

Article DOI:10.21474/IJAR01/11273
DOI URL: http://dx.doi.org/10.21474/IJAR01/11273

RESEARCH ARTICLE

AC BACK SURFACE RECOMBINATION IN N+-P-P+ SILICON SOLAR CELL: EFFECT OF TEMPERATURE

Denise Kabou, Mamadou Lamine Ba, Mamour Amadou Ba, Gora Diop, El Hadji Sow, Oulimata Mballo and Gregoire Sissoko

Manuscript Info

Manuscript History
Received: 05 May 2020
Final Accepted: 10 June 2020
Published: July 2020

Key words:-
Silicon Lamella- Recombination Velocity- Umklapp Process- Optimum Width

Abstract

Excess minority carrier's diffusion equation in the base of monofaciale silicon solar cell under frequency modulation of polychromatic illumination is resolved. Using conditions at the base limits involving recombination velocities Sf and Sb, respectively at the junction (n+/p) and back surface (p+/p), the expression of the excess minority carriers' density δ (T, ω) is determined. The density of photocurrent Jph (T, ω) is represented according to the recombination velocity at the junction for different temperature values. The expression of the ac back surface recombination velocity Sb of minority carriers is then deduced depending on frequency of modulation, temperature, electronic parameters (D) and the thickness of the base. Bode and Nyquist diagrams are used to analyze, both diffusion coefficient and back surface recombination of excess minority carriers submitted to Umklap process.

Copy Right, IJAR, 2020,. All rights reserved.

Introduction:-

The solar cell AC response induced by modulated optical or electrical signal have been used by previous works[1], to determine either the electronics parameters (τ, L, D, Sb)[2],[3], [4]; [5], [6], [7]or the electrical one(Z(ω), G(ω), C(ω), Rs, Rsh)[8], [9], [10]; [11], [12], [13],[14].The externalconditions under which the solar cell is placed are taken into account, in particular, the magnetic field[15], [16], the flow of irradiation by charged particles[17], [18], [19], as well as the temperature[20], [21], [22], [23] and the illuminationwavelength[24], [25].Intrinsic parameters were considered such as, the doping rate of and the geometric parameters[24], [25], [26], [27], [28], [29], [30], [31].

Our work is interested in the n^+-p-p^+ solar cell, under composite illumination in frequency modulation and placed under different temperatures (T), in order to study the AC back surface recombination.

Thus the diffusion coefficient of minority carriers in excess D(ω, T) is represented and analyzed.

The expression of the density of photogenerated carriers is given by the solution of the diffusion equation in the base of the solar cell.

The photocurrent density is then calculated as a function of:

1. surface recombination velocities at the junction (Sf and at the rear (Sb)[32], [33], [34][35],
2. the temperature (T)
3. the illumination modulation frequency (ω) .

Corresponding Author:- Grégoire Sissoko
Address**:-** Laboratory of Semiconductors and Solar Energy, Physics Department, Faculty of Science and Technology, University Cheikh Anta Diop, Dakar, Senegal.

The back recombination velocity expression is deduced as a function of both the temperature (T) and the frequency (ω) of illumination modulation.It is finally analyzed using, the Umklapp process, showing the thermal agitation of charge carriers[23], [36], [37] and the spectroscopy method of Bode and Nyquist diagrams (amplitude and phase).[11], [17], [27], [35], in order to define the electrical circuit modelrepresentation.The real and imaginary parts are plotted versus temperature and modeled through mathematical relationships.

Theory:
The structure of the n^+-p-p^+ monofaciale silicon solar cell[38], [39] under polychromatic illumination, in frequency modulation, is given by figure 1.

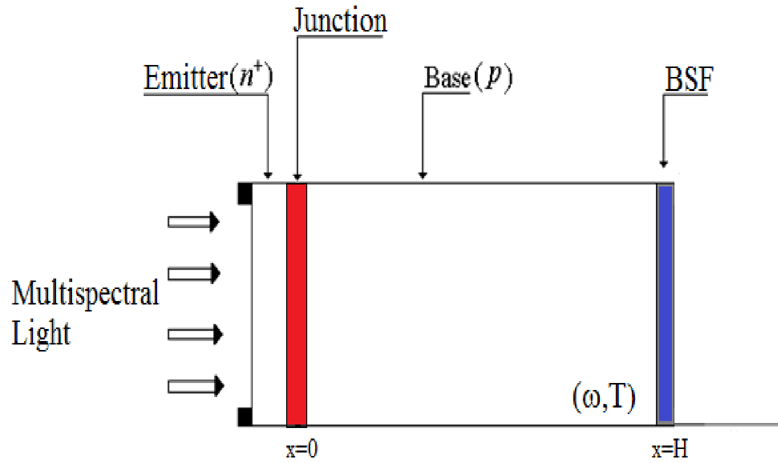

Figure 1:- Structure of monofaciale solar cell.

The excess minority carriers' density $\delta(x,t)$generated in the base of the solar cell obeying to the continuity equation at T temperature, under polychromatic illumination in frequency modulation, is given by [3], [7], [24]:

$$D(\omega,T)\times\frac{\partial^2\delta(x,t)}{\partial x^2}-\frac{\delta(x,t)}{\tau}=-G(x,\omega,t)+\frac{\partial\delta(x,t)}{\partial t} \quad (1)$$

The expression of the excess minority carriers' density is written, according to the space coordinates (x) and the time t, as:

$$\delta(x,t)=\delta(x)\cdot e^{-j\omega t} \quad (2)$$

- Carriers generation rate $G(x,t)$ is given by the relationship [39]:

$$G(x,t)=g(x)\cdot e^{-j\omega t} \quad (3)$$

With:

$$g(x)=\sum_{i=1}^{3}a_i.e^{-b_i.x} \quad (4)$$

- The depth in the base is represented by x.
- Coefficients a_i et b_i are obtained from tabulated values of radiation in AM 1.5 conditions.

- $D(\omega,T)$is the complex diffusion coefficient of excess minority carrier in the base at T temperature. Its expression is given by the relationship [3], [7], [24]:

$$D(\omega,T)=D(T)\times\left(\frac{1-j.\omega^2.\tau^2}{1+(\omega\tau)^2}\right) \quad (5)$$

$D(T)$is the temperature-dependent diffusion coefficient given by Einstein's relationship [20], [22]:

$$D(T) = \frac{\mu(T) \cdot K_b \cdot T}{q} \quad (6)$$

T is the temperature in Kelvin, K_b is the Boltzmann constant:

$$K_b = 1.38 \times 10^{-23} m^2 \cdot Kg \cdot S^{-1} \cdot K^{-1}$$

The mobility coefficient [20] for electrons, expressed according to the temperature, is given by:

$$\mu(T) = 1.43 \cdot 10^{19} T^{-2.42} \quad (7)$$

By replacing equations (2) and (3) in equation (1), the continuity equation for the excess minority carriers' density in the base is reduced to the following relationship:

$$\frac{\partial^2 \delta(x,\omega)}{\partial x^2} - \frac{\delta(x,\omega)}{L^2(\omega,T)} = -\frac{g(x)}{D(\omega,T)} \quad (8)$$

$L(\omega,T)$ is the complex diffusion length of excess minority carriers in the base given by :

$$L(\omega,T) = \sqrt{\frac{D(\omega,T)\tau}{1 + j\omega\tau}} \quad (9)$$

τ isthe excess minority carriers lifetime in the base.

1) The solution of equation (8) is:

$$\delta(x,\omega,T) = A \cdot \cosh\left[\frac{x}{L(\omega,T)}\right] + B \cdot \sinh\left[\frac{x}{L(\omega,T)}\right] + \sum K_i \cdot e^{-b_i \cdot x} \quad (10)$$

With $K_i = -\frac{a_i \cdot [L(\omega,T)]^2}{D(\omega,T)\left[L(\omega,T)^2 \cdot b_i^2 - 1\right]}$

and $\left(L(\omega,T)^2 \cdot b_i^2 \neq 1\right)$ (11)

Coefficients A and B are determined through the boundary conditions:

- At the junction (x = 0)

$$D(\omega,T)\left.\frac{\partial \delta(x,T)}{\partial x}\right|_{x=0} = Sf \cdot \left.\frac{\delta(x,T)}{D(\omega,T)}\right|_{x=0} \quad (12)$$

- On the back side in the base (x = H)

$$D(\omega,T)\left.\frac{\partial \delta(x,T)}{\partial x}\right|_{x=H} = -Sb \cdot \left.\frac{\delta(x,T)}{D(\omega,T)}\right|_{x=H} \quad (13)$$

Sf and Sb are respectively the recombination velocities of the excess minority carriers at the junction and at the back surface. The recombination velocity Sf reflects the charge carrier's velocity crossing the junction, in order to contribute to the photocurrent. It is then related to the external load which imposes the solar cell operating point [30], [32], [33]. It has an intrinsic component which produces the carrier losses associated with the shunt resistor in the solar cell electrical equivalent model [17], [19] [34)]. The excess minority carrier recombination velocit0y Sb on the back surface is associated with the presence of the p^+ layer which produces an electric field for returning back the charge carriers' accross the junction [38], [40], [41], [42].

Results and Discussions:-

Diffusion Coefficient: Bode and Nyquist Diagrams at Different Temperatures:

The amplitude and phase of the diffusion coefficient under different temperature are represented versus frequencythrough figures 2 and 3.

For a given temperature, the effective diffusion coefficient is maximum and constant when the frequency is low(steady state). In a dynamic frequency regime, the repeated excitations of excess minority carriers lead to a relaxation problem that slows their diffusion and bringht out a negative phase of the diffusion coefficient. Indeed, the diffusion of minority carriers decreases with an increase in temperature.The effective diffusion coefficient is more sensitive to temperature in a quasi-static regime.

The Nyquist diagram is shown in figure 4.

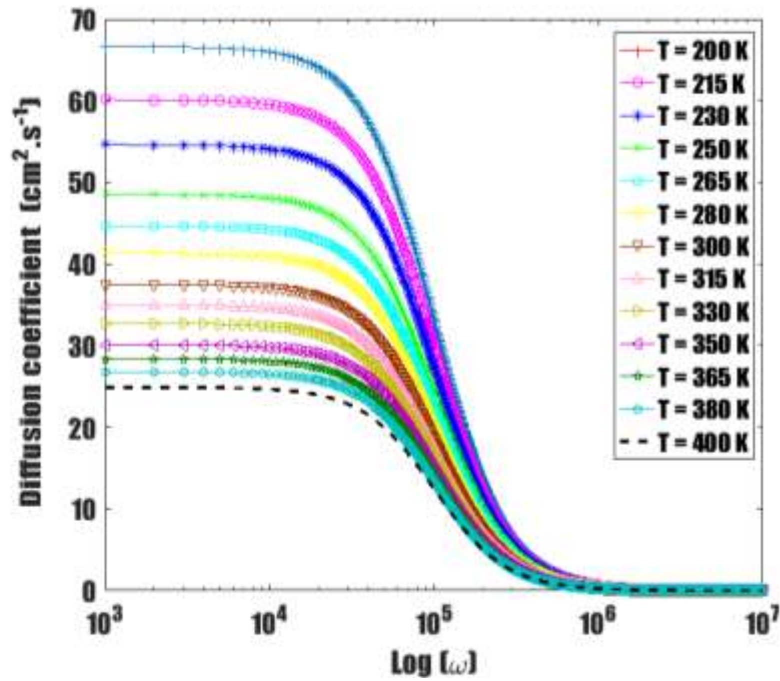

Figure 2:- Diffusion coefficient versus frequency for different temperatures.

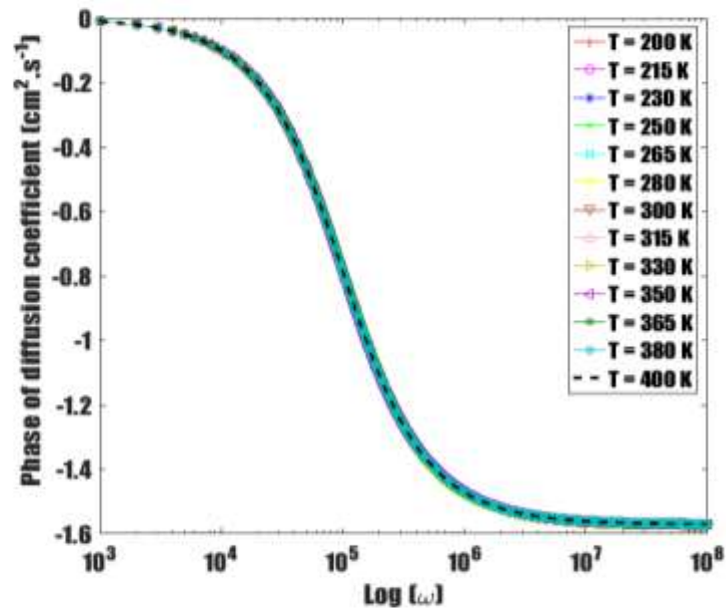

Figure 3:- Diffusion coefficient phase versus frequency for different temperatures.

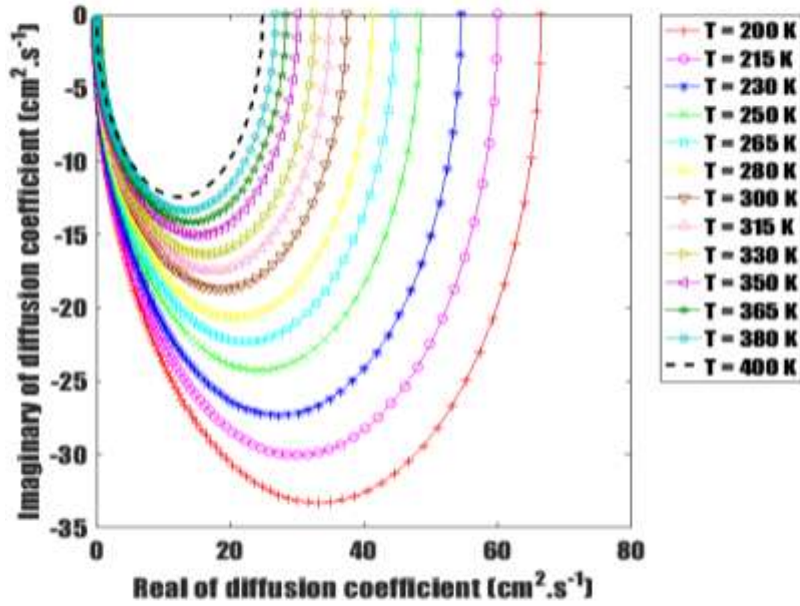

Figure 4:- Imaginary component versus real component of diffusion coefficient for different temperatures.

We find that the radius of the semicircles decreases according to the temperature with a shift from the center of the circles towards the origin of the axes. The semi-circle has no shift at the origine of axes, indicates then a resistor(Rp) in parallel with a capacitor(C)[11], [43], [45], [46] and so gives rise to a single time constant(Rp.C), temperature dependent. The investigation of the half-circle radius, thus suggests electrical parameters characteristic leading to equivalent electric model[11],[27], [35], [28].

Minority carrier'sdensity for different frequencies and temperatures:

The figures. 5, 6 and 7, give the profile of the density of minority carriers in excess with the depth of the base, for different frequencies and at a given temperature.

Figure 5 shows an amplitude of density of minority carriers in excess that is increasing with temperature, and is insensitive to low frequencies (steady state in amplitude of effective diffusion coefficient)

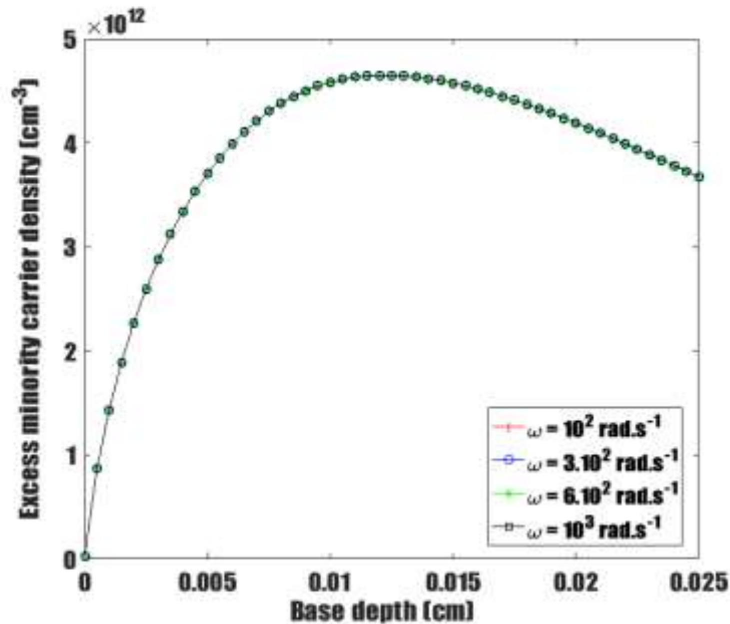

Figure 5:- Excess minority carrier's density versus base depth for different frequencies (T=200 K)

At low temperatures (Fig. 6), the amplitude of the density of minority carriers in excess decreases due to the low thermal agitation and remains sensitive to variations in frequency (region of abrupt variation of the diffusion coefficient).

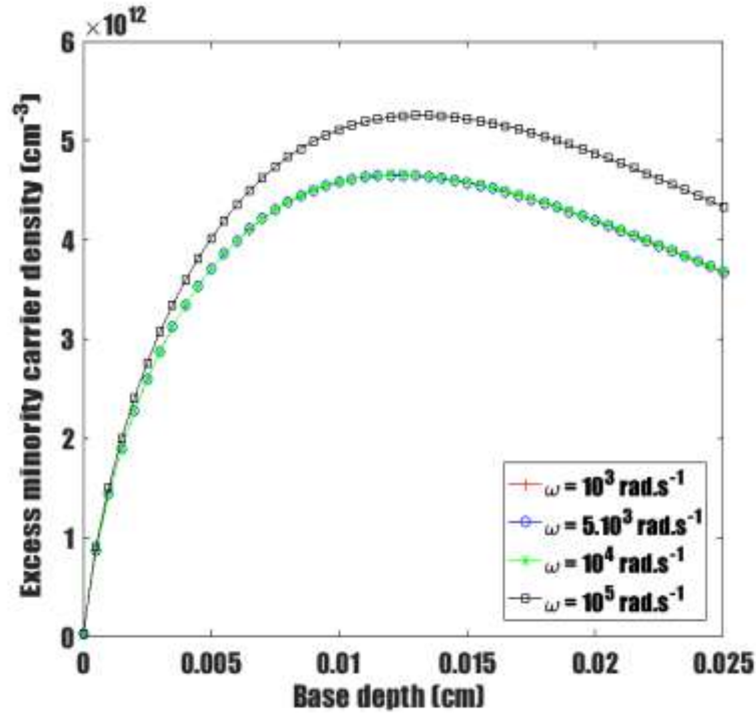

Figure 6:- Excess minority carrier's density versus base depth for different frequencies (T=200 K).

When temperature increases, the density of excess carriers undergoes thermal agitation, by increasing amplitude (Umklap process) and variation in frequency (in stationary zone) is insensitive (Fig. 7) [36], [37].

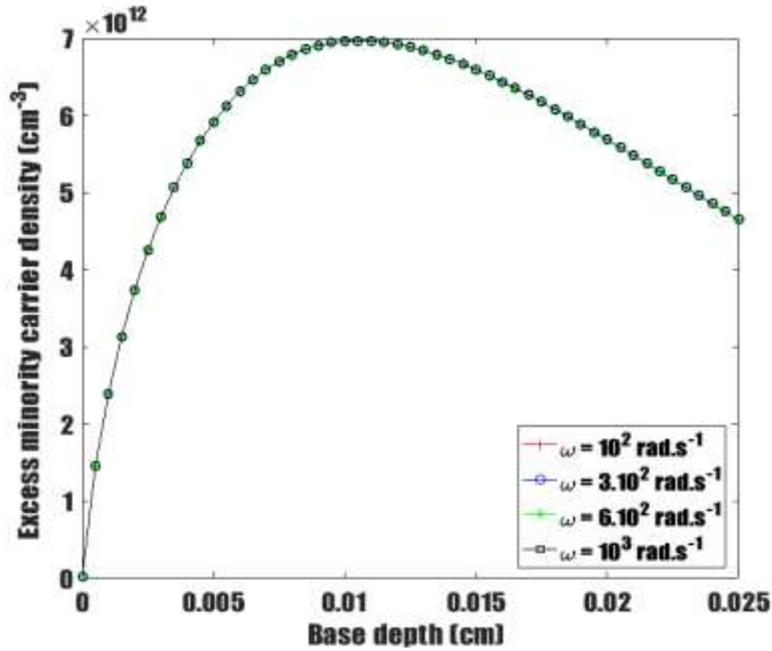

Figure 7:- Excess minority carrier's density versus base depth for different frequencies (T=300 K).

In Figure 8, in addition to the high temperature requiring greater thermal agitation of the minority carriers, the increase in frequency on the other hand cecreases the amplitude of the density of the carriers with the base depth [21], [23], [36], [37].

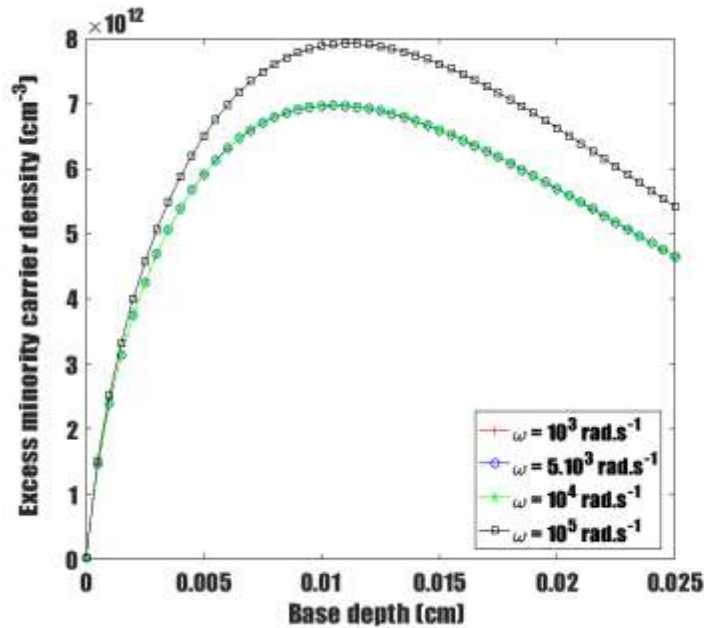

Figure 8:- Excess minority carrier's density versus base depth for different frequencies (T=300 K)

Photocurrent:

The density of photocurrent at the junction is obtained from the density of minority carriers in the base and is given by the following expression:

$$J_{ph}(Sf, Sb, \omega, T) = qD(\omega, T)\left.\frac{\partial\delta(x, Sf, Sb, \omega, T)}{\partial x}\right|_{x=0} \tag{14}$$

Where q is the elementary electron charge.

Figure 5 shows ac photocurrent versus the junction surface recombination velocity for different temperatures.

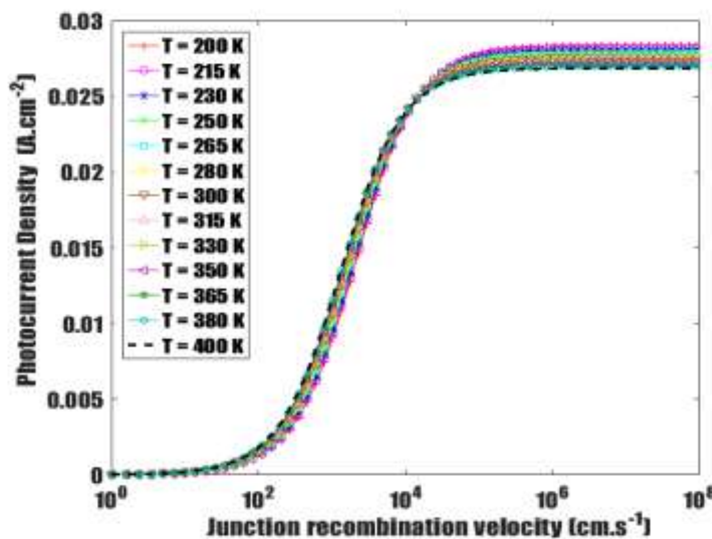

Figure 9:- Photocurrent density versus junction surface recombination velocity for different temperatures (**ω**=10^5 rad/s).

Deduction of the Sb (ω, T) expression:
The representation of photocurrent density (**figure. 9**) according to the junction recombination velocity of minority carriers shows that, for very large Sf, a bearing sets up and corresponds to the short-circuit current density (Jphsc). So, in this junction recombination velocity interval, it comes [30], [32], [33], [34]:

$$\left.\frac{\partial J_{ph}(Sf, Sb, \omega, T)}{\partial Sf}\right|_{Sf \geq 10^5\, cm.s^{-1}} = 0 \quad (15)$$

The solution of the above equation leads to expressions of the ac recombination velocity in the back surface, given as:

$$Sb1(\omega,T) = \frac{D(\omega,T)}{L(\omega,T)} \sum_{i=1}^{3} \frac{L(\omega,T).b\left(\exp(-bi.H) - \cosh\left(\frac{H}{L}\right)\right) - \sinh\left(\frac{H}{L}\right)}{L(\omega,T)\cdot bi \cdot \sinh\left(\frac{H}{L(\omega,T)}\right) + \cosh\left(\frac{H}{L(\omega,T)}\right) - \exp\left(-bi.H\right)} \quad (16)$$

$$Sb2(\omega,T) = -\frac{D(\omega,T)}{L(\omega,T)}.\tanh\left(\frac{H}{L(\omega,T)}\right) \quad (17)$$

Previous works have investigated at the second solution (Eq. 17) [27], [28]. Our study will deal with this second solution whose module and phase are represented versus logarithm of the modulation frequency by figures 6 and 7, for different temperature values.

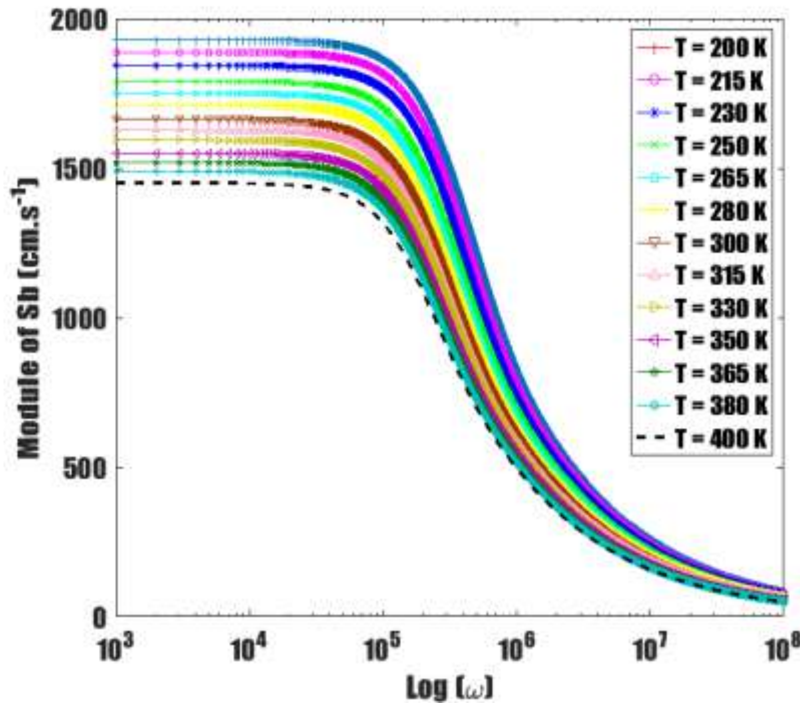

Figure 10:- Module of Sb versus frequency for different temperatures.

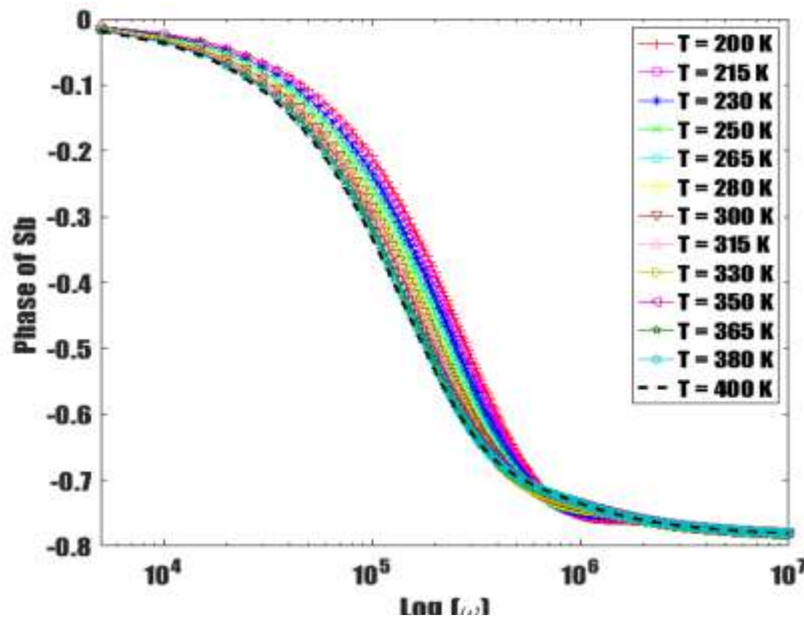

Figure 11:- Phase of Sb versus frequency for different temperatures.

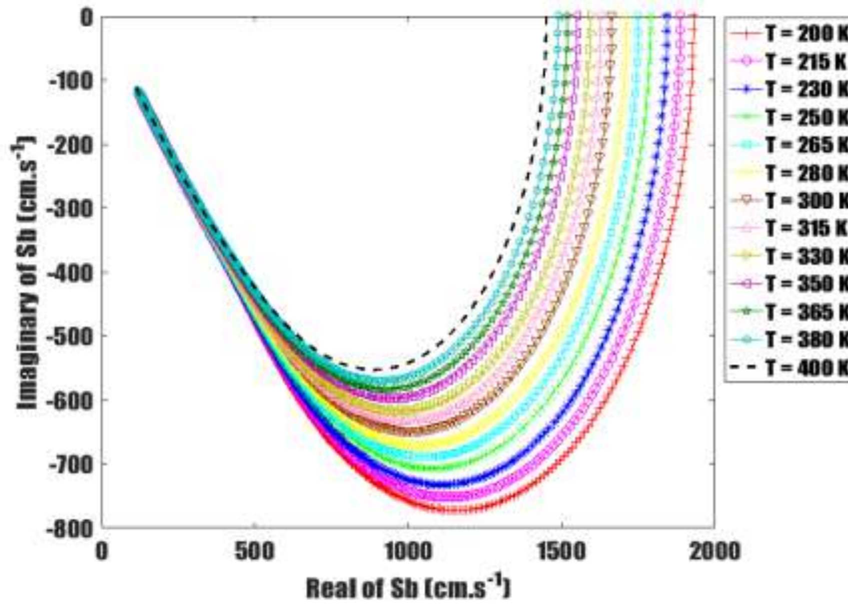

Figure 12:- Imaginary component versus real component of Sb for different temperatures.

Ac Sb in complex form (real and imaginary components, with J complex number) is presented by analogy with Maxwell-Wagner-Sillars (MWS) model [43], [44], [45], [46] and can be written as:

$$Sb(\omega,T) = Sb'(\omega,T) + J \cdot Sb''(\omega,T) \quad (18)$$

Ac phase (T) for a given temperature , is written as:

$$\tan(\phi(\omega,T)) = \frac{Sb''(\omega,T)}{Sb'(\omega,T)} \quad (19)$$

Sb_{ampl} (ω, T) and ϕ (ω, T) correspond for a given temperature T, to the amplitude and phase component of Sb.
At low frequencies ($\leq 10^4$ rad/s), the stationary regime is observed and gives constant amplitudes that decrease with the temperature T (**figure. 10**).

Beyond the frequency (≫10^4 rad/s), the cut-off frequency (ω_c, Sb (T)) is determined for each temperature. It is noted that the cut-off frequency decreases with the temperature T, as does the amplitude (Sb_{ampl})(See **Table. 1**).

The phase is negative for all values of the frequency and decreases slighly with the temperature T(**figure. 11**).
Figure. 12 represents the Niquyst diagram of the excess minority carriers recombiation velocity for different temperatures. The redius of the semi-circles decrease with the temperature (See table 2 and table 3).

Figure 10 and figure 11 show that the sb recombination velocity decreases with temperature. Indeed, when the temperature is above the optimum temperature (Topt-300 K) [37], thermal agitation yealds to the exponential evolution of umklapp processes that predict a temperature dependence of thermal conductivity in 1/T [23] [37]. This decreases the mobility of excess minority carriers and results in a decrease in the effective diffusion coefficient [23], [35] which increases recombination.

The negative phase of the ac Sb recombination velocity and the determination of electrical parameters, with the Bode and Nyquist diagrams, characterizing Sb, allow to determine the equivalent electric model [1], [11], [27], [28], [44].

Table 1:- Ac Sb cut-off frequency for different temperature values.

T (K)	200	215	230	250	265	280	300	315	330	350	365	380	400
ω_c (10^5rad/s)	1.58	1.52	1.35	1.31	1.21	1.16	1.02	1.01	$9.5.10^4$	$9.4.10^4$	9.10^4	$8.7.10^4$	$8.5.10^4$
Sb (T)	1784	1736	1710	1648	1619	1582	1552	1514	1487	1440	1414	1387	1349
Sbampl	1930	1887	1844	1790	1751	1713	1663	1628	1594	1551	1519	1489	1450
ω(10^5rad/s)	$1.3.10^4$	10^4	$1.2.10^4$	9.10^3	5.10^3	3.10^3	9.10^3	8.10^3	7.10^3	4.10^3	8.10^3	6.10^3	8.10^3

Table 2:- Maximum amplitude of the imaginary part of Sb for different temperature values.

T (K)	200	215	230	250	265	280	300	315	330	350	365	380	400
$ImSb_{max}(cm/s^1)$	464.58	451.70	431.88	417.17	404.36	392.10	372.74	366.67	357.03	344.79	336.19	328.33	313.52

Table 3:- Maximum amplitude of real partof Sb for different temperature values.

T (K)	200	215	230	250	265	280	300	315	330	350	365	380	400
$Re(Sb(cm.s^1)$	1873.25	1832.14	1792.71	1740.71	1703.67	1667.52	1620.69	1586.17	1553.5	1512.19	1481.33	1452.35	1415.7
$\left(\frac{1}{Re(Sb(cm.s^{-1}))}\right)\times 10^{-5}$	53.38	54.58	55.78	57.45	58.70	59.97	61.70	63.04	64.37	66.13	67.51	68.85	70.64

Conclusion:-

The solar cell's ac back surface (p/p^+) recombination velocity that controls the recombination of the excess minority carriers has been determined. Thus, the spectroscopy method allowed the study of the Bode and Nyquist diagrams and extracted certain electrical parameters characterizing the equivalent electric model. The effect of temperature on back surface recombination velocity was explained by umklapp processes.

References:-

1. D. Vanmaekelbergh and F. Cardon (1992). Recombination in semiconductor electrodes investigation by the electrical impedance. Electrochimica Acta. Vol. 37 N0 5. Pp. 837-846
2. Wang, C.H. and Neugroschel, A. (1987) Minority-Carrier Lifetime and Surface Recombination Velocity Measurement by Frequency-Domain Photpluminescence. IEEE Transaction on Electron Devices, 38, 2169-2180. http://dx.doi.org/10.1109/16.83745
3. Konstantinos Misiakos and Dimitris Tsamakis (1994). Electron and Hole Mobilities in Lightly Doped Silicon. Appl. Phys. Lett. 64(15), pp.2007-2009.
4. 4.Th. Flohr and R. Helbig, (1989) Determination of minority-carrier lifetime and surface recombination velocity by Optical-Beam-Induced- Current measurements at different light wavelengths J. Appl. Phys. Vol.66 (7), pp 3060 – 3065.
5. R. R. Vardanyan, U. Kerst, B. Tierock, H. G. Wagemann(1997). Measurement of recombination parameters of solar cell in a magnetic field. Proceeding of the 14th European Photovoltaic Solar Energy Conference (Barcelona, Spain). Pp 2367-2369.

6. Sudha Gupta, Feroz Ahmed and Suresh Garg, (1988) A method for the determination of the material parameters τ, D, L_o, S and α from measured A.C. short-circuit photocurrent Solar Cells, Vol. 25, pp 61-72
7. Luc Bousse, Shahriar Mostarshed, Dean Hafeman, Marco Sartore, Manuela Adami and Claudio Nicolini (1994). Investigation of carrier transport through silicon wafers by photocurrent measurement. J. Appl. Phys. 75 (8), pp.4000- 4008.
8. John H. Scofield (1995). Effects of series and inductance on solar cell admittance measurements. Solar Energy and Solar Cells, 37 (2), 217- 233.
9. Gokhan Sahin, Moustapha Dieng, Mohamed Abderrahim Ould El Moujtaba, Moussa 1ibra Ngom, Amary Thiam, Grégoire Sissoko (2015). Capacitance of vertical parallel junction silicon solar cell under monochromatic modulated illumination. Journal of Applied Mathematics and Physics, 3, pp. 1536-1543.
10. Liu, J.J. and Wong, W.W. (1992) Comparison and Optimization of the Performance of Si and GaAs Solar Cells. Solar Energy Materials and Solar Cells, 28, 9-28. http://dx.doi.org/10.1016/0927-0248(92)90104-
11. R. Anil Kumar, M.S. Suresh and J. Nagaraju (2001). Measurement of AC parameters of gallium Arsenide (GaAs/Ge) solar cell by impedance spectroscopy. IEEE Transaction on Electron Devices, Vol. 48, N0 9, pp 2177-2179.
12. R. L. Streever; J. T. Breslin and E. H. Ahlstron (1980). Surface states at the n-GaAs-SiO2 interface from conductance and capacitance measurements. Solid State Electronics Vol. 23, pp. 863-868.
13. Giora Yaron and Dov Frohman-Bentchrowsky (1980). Capacitance voltage characterization of poly Si-SiO_2-Si structures. . Solid State Electronics Vol. 23, pp. 433-439.
14. Zbigniew Razimski, Jeffrey Honneycut and George A. Rozgoni (1988). Minority carrier lifetime analysis of silicon epitaxy and bulk crystals with nonuniformly distribute defects. IEEE Transaction on Electron Devices, Vol. ED-35, N0 1, pp 80-84.
15. A. Dieng, A. Diao, A.S. Maiga, A. Dioum, I. Ly, G. Sissoko (2007). A Bifacial Silicon Solar Cell Parameters Determination by Impedance Spectroscopy. Proceedings of the 22nd European Photovoltaic Solar Energy Conference and Exhibition-Italy (2007), pp.436-440
16. Ali Moissi, Martial Zoungrana, Abdourrahmane Diallo, Senghane Mbodji, Hawa Ly Diallo, Ali Hamidou, Mor Ndiaye and Grégoire Sissoko (2014). Base Transceiver Station (BTS) Antenna Electric Field Influence on the Space ChargeRegion in a Silicon Solar Cell. Research Journal of Applied Sciences, Engineering and Technology, 7(12): 2554-2558,
17. El Hadji Ndiaye, Gokhan Sahin, Moustapha Dieng, Amary Thiam, Hawa Ly Diallo, Mor Ndiaye, Grégoire Sissoko (2015). Study of the intrinsic recombination velocity at the junction of silicon solar cell under frequency modulation and radiation Journal of Applied Mathematics and Physics, 2015, 3, 1522-1535 Published Online November 2015 in SciRes. http://www.scirp.org/journal/jamp http://dx.doi.org/10.4236/jamp.2015.311177.
18. Mohamadou Samassa Ndoye, Boureima Seibou, Ibrahima Ly, Marcel Sitor Diouf, Mamadou Wade, Senghane Mbodji, Grégoire Sissoko(2016). Irradiation Effect on Silicon Solar Cell Capacitance in Frequency Modulation. International Journal of Innovative Technology and Exploring Engineering (IJITEE) ISSN: Volume-6 Issue-3, pp. 2278-3075.
19. Fatimata Ba, boureima Seibou, mamadou Wade, marcel Sitor Diouf, brahima Ly and grégoire Sissoko (2016).Equivalent Electric Model of the Junction Recombination Velocity limiting the Open Circuit of a Vertical Parallel Junction Solar Cell under Frequency Modulation. IPASJ International Journal of Electronics & Communication (IIJEC), Volume 4, Issue 7, pp.1-11.
20. M. Kunst, G. Muller, R. Schmidt and H. Wetzel (1988). Surface and volume decay processes in semiconductors studied by contact lesss transient photoconductivity measurelments Appl. Phys. Vol. 46, pp77-85.
21. Diatta. I., Ly. I., Wade. M, Diouf. M.S, Mbodji. S. and Sissoko. G (2016). Temperature Effect on Capacitance of a Silicon Solar Cell under Constant White Biased Light World. Journal of Condensed Matter Physics, 6, 261-268. http://www.scirp.org/journal/wjcmp
22. N.D. Arora, J. R. Hauser, D. J. Roulston (1982). Electron and hole mobilities in silicon as a function of concentration and temperature. IEEE. Trans. Electron devices, vol. ED-29, pp.292-295.
23. Richard Mane, Ibrahima Ly, Mamadou Wade, Ibrahima Datta, Marcel S. Douf, Youssou Traore, Mor Ndiaye, Seni Tamba, Grégoire Sissoko (2017). Minority Carrier Diffusion Coefficient D*(B, T): Study in Temperature on a Silicon Solar Cell under Magnetic Field. Energy and Power Engineering, 9, pp.1-10 http://www.scirp.org/journal/epe
24. Mandelis, A.A. Ward and K.T. Lee.(1989). Combined AC photocurrent and photothermal reflectance response theory of semiconducting p-n junctions. J. Appl. Phys. Vol.66. No.11. pp 5572 – 5583. http://dx.doi.org/10.1063/1.343662

25. Antilla O. J., Hahn S. K. (1993). Study on surface photovoltage measurement of long diffusion length silicon: simulation results. J. Appl. Phys. 74(1), pp.558-569.
26. D. L. Meier., J.-M. Hwang and R. B. Campbell (1988).The effect of doping density and injection level on minority-carrier lifetime as applied to bifacial dendritic web silicon solar cells. IEEE Transactions on Electron Devices, 35(1), 70–79.
27. Y. Traore, N. Thiam, m. Thiame, M. L. Ba, M. S. Diouf et G. Sissoko (2019). AC Recombination Velocity in the Back Surface of a Lamella Silicon Solar Cell under Temperature.Journal of Modern Physics, vol. 10, pp. 1235-1246.
28. M. Gueye, H. L. Diallo, A. Kosso, M. Moustapha, Y. Traore, I. Diatta et G. Sissoko(2018). Ac Recombination Velocity in a Lamella Silicon Solar Cell. World Journal of Condensed Matter Physics, vol. 8, pp. 185-196,http://www.scirp.org/journal/wjcmp.
29. Honma, N. and C. Munakata, 1987. Sample thickness dependence of minority carrier lifetimes measured using an ac photovoltaic method. Jap. J. Appl. Phys., 26(12): 2033-203.
30. Diallo. H.L, Seïdou. A. Maiga, Wereme. A and Sissoko G (2008). New Approach of Both Junction and Back Surface Recombination Velocities in a 3D Modelling Study of a Polycrystalline Silicon Solar Cell. The European Physical Journal Applied Physics, 42, pp.203-211. https://doi.org/10.1051/epjap:2008085
31. Fatoumata Baldé, Hawa Ly Diallo, Hamet Yoro Ba, Youssou Traoré, Ibrahima Diatta, Marcel SitorDiouf,MamadouWade,GrégoireSissoko (2018). Externalelectricfieldasappliedtodeterminesilicon solar cell space charge region width. Journal of Scientific and, Engineering Research, (JSER), 5(10):252-259, ISSN: 2394-2630.
32. G. Sissoko, C. Museruka, A. Corréa, I. Gaye and A. L. Ndiaye (1996). Light spectral effect on recombination parameters of silicon solar cell. Renewable Energy, Vol 3, pp.1487-1490. Pergamon, 0960-1481
33. G. Sissoko, E. Nanéma, A. Corréa, P. M. Biteye, M.Adj, A. L. Ndiaye (1998). Silicon Solar cell recombination parameters determination using the illuminated I-V characteristic. Renewable Energy, vol-3, pp.1848-51-Elsevier Science Ltd, 0960-1481/98/#.
34. Ly Diallo. H, Wade. M, Ly. I., Ndiaye. M, Dieng. B, O. H. Lemrabott, A.S. and Maiga Sissoko. G (2012). 1D Modeling of a Bifacial Solar Cell Silicon under Monochromatic Illumination Frequency Modulation: Determination of the Equivalent Electrical Circuit Related to the Recombination Area Velocity. Research Journal of Applied Sciences, Engineering and Technology, 4, 1672-1676.
35. Mint Sidihanena Selma, Ibrahima DIATTA, Youssou TRAORE, Marcel Sitor DIOUF, Lemrabottould Habiboulahh, Mamadou WADE, Grégoire SISSOKO (2018). Diffusion capacitance in a silicon solar cell under frequency modulated illumination: Magnetic field and temperature effects, , Journal of Scientific and Engineering Research, 5(7):317-324, Available online www.jsaer.com
36. Thurmond (1975). The standard thermodynamic functions for the formation of electron and hole in Ge, Si, GaAs and GaP. J. Electrochem. Soc, vol. 122, pp.133-41.
37. Berman, R. (1951) Thermal Conductivity of Dielectric Crystals: The “Umklapp”. Nature, 168, 277-280.
38. Le Quang Nam, M. Rodot, M. Ghannam, J. Cppye, P. de Schepper, J. Nijs, (1992). Solar Cells with 15.6% efficiency on multicristalline silicone, using impurity gettering, back surface field and emitter passivation. Int. J. Solar Energy. Vol. 11, pp.273-279.
39. Fossum. J.G (1977). Physical Operation of Back-Surface-Field Silicon Solar Cells. IEEE Transactions on Electron Devices, 2, 322-325. https://doi.org/10.1109/T-ED.1977.18735
40. Furlan, J. and Amon, S. (1985) Approximation of the Carrier Generation Rate in Illuminated Silicon. Solid State Electronics, 28, pp.1241-1243. https://doi.org/10.1016/0038-1101(85)90048-6
41. Joardar. K., Dondero. R.C. and Schroda. D.K (1989). Critical Analysis of the Small-Signal Voltage-Decay Technique for Minority-Carrier Lifetime Measurement in Solar Cells. Solid State Electronics, 32, pp.479-483.
42. B. H. Rose And H. T. Weaver, Determination of effective surface recombination velocity and minority-carrier lifetime in high-efficiency Si solar cells , J. Appl. Phys . 54. Pp 238-247, (1983)
43. J. C. Maxwell, Electricity and magnetism (1982) .Calerdon, Oxford, 1.
44. B. Lestriez, A. Maazouz, Is the Maxwell-Sillars-Wagner model reliable for describing the dielectric properties of a core Shell particle- epoxy system, Polymer 39, 6733-6742 (1998).
45. C. J. F. Bottcher, P. Bordewijik, Theory of electric polarization (1979). Adv. Mol. Relax. Inter. Proces. 14, 161-162.
46. S. Havriliak, S. Negami, A complex plane representation of dielectric and mechanical relaxation processes in some polymers(1967). Polymer 8, 161-210.